

## STUDY OF ULTRATHIN PRUSSIAN BLUE FILMS USING IN SITU ELECTROCHEMICAL SURFACE PLASMON RESONANCE

Stelian LUPU<sup>a</sup>, Laura PIGANI<sup>b1</sup>, Renato SEEBER<sup>b2,\*</sup>, Fabio TERZI<sup>b3</sup> and Chiara ZANARDI<sup>b4</sup>

<sup>a</sup> Department of Analytical Chemistry and Instrumental Analysis, University Politehnica of Bucharest, Polizu Gheorghe 1-3, 011061 Bucharest, Romania; e-mail: s\_lupu@chim.upb.ro

<sup>b</sup> Department of Chemistry, University of Modena e Reggio Emilia, via G. Campi 183, 41100 Modena, Italy; e-mail: <sup>1</sup>lpigani@unimore.it, <sup>2</sup>seeber.renato@unimore.it,

<sup>3</sup>fterzi@unimore.it, <sup>4</sup>czanardi@unimore.it

Received July 27, 2004

Accepted January 5, 2004

Characterisation of ultrathin Prussian Blue films has been performed using in situ electrochemical surface plasmon resonance technique. Prussian Blue films have been prepared by potentiostatic method on a gold-coated glass surface plasmon resonance sensor. The electrochemical reduction of Prussian Blue to Prussian White and oxidation to Berlin Green are accompanied by a change of the refractive index; the system shows repeating voltammetric responses over subsequent potential cycles. The surface plasmon resonance signal is capable of evidencing minute electrochemically induced changes in the inorganic film coating the electrode.

**Keywords:** Surface plasmon resonance; Prussian Blue; Modified electrodes; Ultrathin films; Cyclic voltammetry; Chronoamperometry; Electrodeposition; Electrochemistry.

The application of non-conventional techniques to the study of the formation and of the electrochemical properties of films on electrode surfaces is of key importance for preparation and use of new sensors based on modified electrodes. In order to achieve a better understanding of the electrochemical processes on which these devices are based, many analytical techniques have been used, such as controlled potential methods, electrochemical impedance measurements, electrochemical microgravimetry (quartz crystal microbalance)<sup>1</sup>, and spectroelectrochemical techniques. In recent years, surface plasmon resonance<sup>2,3</sup> (SPR) has proved to be a highly sensitivity technique for characterising ultrathin films and for monitoring very small changes at the electrode|electrolyte solution interface<sup>4-7</sup>.

Among different modifiers of electrode surface, metal hexacyanoferrates have attracted much interest<sup>8,9</sup>. Prussian Blue (PB), i.e. iron(III) hexacyano-

ferrate, is probably the most extensively studied inorganic modifier, due to its electrochromic properties, electrocatalytic activity, and chemical stability in acidic aqueous solutions. PB has been used in the electrocatalytic reduction of  $\text{CO}_2^{10}$  and of  $\text{H}_2\text{O}_2^{11}$ , and in the oxidation of hydrazine<sup>12</sup>, ascorbic acid, and dopamine<sup>13,14</sup>. Furthermore, the thermodynamics of redox systems in which PB is involved is of high interest when considering bilayer electrode coatings<sup>15,16</sup>.

This work deals with the *in situ* monitoring of the redox behaviour of ultrathin PB films using electrochemical SPR (ESPR); in such a technique, different potential waveforms are applied on the modified electrode and electrochemical (current) and optical data are simultaneously collected. Ultrathin PB films have been prepared by a potentiostatic method on gold-coated glass sensors. The ESPR characterisation has been performed in different aqueous media, in order to check the capability of detecting possible effect of the medium on the stability of these ultrathin films. ESPR has proved to be an interesting and valuable tool to achieve new insights into microscopic changes of the electrode|modifier|electrolyte interfaces. However, in the case of PB, theoretical models have not been developed in the literature in order to give a rationale to the correlations between SPR signals and structure.

## EXPERIMENTAL

### Chemicals

All chemicals:  $\text{FeCl}_3 \cdot 6\text{H}_2\text{O}$  (Carlo Erba),  $\text{K}_3[\text{Fe}(\text{CN})_6]$  (Aldrich),  $\text{KCl}$  (Acros),  $\text{K}_2\text{SO}_4$  (Carlo Erba),  $\text{KClO}_4$  (Carlo Erba),  $\text{KNO}_3$  (Riedel de Häen),  $\text{HCl}$  (Riedel de Häen) and  $\text{H}_2\text{SO}_4$  (Riedel de Häen) were used as received. De-ionised water (Millipore) was always used to prepare aqueous solutions for electrochemical use.

### Electrochemical Surface Plasmon Resonance

Electrochemical experiments were carried out with an Autolab PGSTAT 12 potentiostat-function generator electrochemical instrument (Ecochemie, Utrecht, The Netherlands) coupled with an ESPR instrument (Autolab Esprit, Ecochemie, Utrecht, The Netherlands). The surface plasmon resonancy is a quantum optical-electrical phenomenon based on the interaction between an incident radiation and a metal surface<sup>2,3</sup>. A light beam can be completely reflected at the interface between two materials with a different refractive index when the incidence angle exceeds a critical angle (total internal reflection, TIR). In particular, this process has been observed when a light beam, propagating inside a glass prism, reaches the interface between the glass and a solution in contact with the prism. This arrangement (Kretschmann configuration) is mostly used in analytical systems. If a thin metal layer is deposited on the glass surface, the light beam can transfer its energy to free electrons loosely bound to the metal atoms. Many metals can be used for the coating; gold is the most used

for analytical purposes due to the resistance to oxidation. The photon/electron interactions generate an evanescent wave, propagating few tens or hundreds of nanometers into the solution. The energy transfer occurs at a specific angle and energy of the photon (resonance conditions). The plot of the intensity of the reflected beam vs the reflectance angle shows a minimum corresponding to resonance conditions. The presence of a thin layer of adsorbed molecules on the surface of gold leads to a change in the resonance conditions; in particular, the position of the minimum depends on the thickness and on optical properties, in particular on the refractive index and dielectric constant, of adsorbed species.

In the Autolab Esprit instrument the light source is a laser (670 nm) and the radiation is p-polarized; the light beam is focused on a thin layer of gold (ca. 50 nm) deposited on BK-7 glass with Ti (ca. 1.5 nm) interface, where the Ti layer improves the adhesion of Au film. The instrument can measure the dependence of intensity of the reflected light versus reflectance angle or versus time at a fixed angle. In this article results are expressed in terms of shift of the minimum with respect to the bare gold substrate immersed in the testing solutions, at varying potential or with time at constant potential. Reflectance is expressed as the ratio between intensities of reflected and incident beam, respectively.

The gold-coated glass surface SPR probe was employed as a working electrode; the silver–silver chloride electrode as a reference electrode, and the platinum rod served as an auxiliary electrode. All potential values were related to the Ag|AgCl reference. Before each electrochemical experiment the surface of the working electrode was washed with ethanol (96%) and then allowed to dry at room temperature. Films were removed from the working electrode surface by dipping them into 3 M KOH solution and then washed carefully with distilled water, acetone, and finally with ethanol (96%).

#### Deposition Procedure of PB Films

Prussian Blue was deposited onto the electrode by a potentiostatic method at potential +0.40 V, from freshly prepared aqueous solutions containing  $K_3[Fe(CN)_6]$  and  $FeCl_3$  in equal concentrations, and  $HCl$  or  $K_2SO_4$  and  $H_2SO_4$  as supporting electrolytes.

The thickness ( $d$ ) of the PB film was estimated according to<sup>17,18</sup>, using Eq. (1):

$$d = \frac{QI^3N_A}{4nFA}, \quad (1)$$

where  $Q$  is the charge consumed for deposition,  $I$  the length of the PB unit cell<sup>19</sup> in cm ( $I = 10.26 \times 10^{-8}$  cm),  $N_A$  the Avogadro constant,  $n$  the number of electrons ( $n = 1$  in our case),  $F$  the Faraday constant, and  $A$  the area of the sensing surface coated with the PB film in  $cm^2$  ( $A = 0.071$   $cm^2$  in our case). Typical thickness of freshly deposited films ranges between 6 and 30 nm. After deposition, the modified electrode was rinsed with fresh electrolyte solution flowing through the SPR cuvette. The characterisation of the film was performed in aqueous solutions containing various supporting electrolytes:  $KCl$  and  $HCl$ , or  $K_2SO_4$  and  $H_2SO_4$ , or  $KNO_3$ .

## RESULTS AND DISCUSSION

Prussian Blue has been described by two formulations, i.e. the soluble form,  $KFe^{III}[Fe^{II}(CN)_6]$ , and the insoluble form, i.e.  $Fe_4^{III}[Fe^{II}(CN)_6]_3$ . Both compounds are actually insoluble, the solubility being in both cases lower than  $10^{-6}$  mol l<sup>-1</sup>; the denomination soluble and insoluble refers actually to the ease of the peptisation of the potassium compound.

It has been suggested that freshly deposited films are in the insoluble form and during the initial electrochemical cycling in K<sup>+</sup>-containing solutions a portion of the film is converted into the soluble form<sup>20,21</sup>. Furthermore, PB may be converted into Prussian White (PW) by reduction to the Fe<sup>II</sup>-Fe<sup>II</sup> system and oxidised to Berlin Green (BG), i.e., to the corresponding Fe<sup>III</sup>-Fe<sup>III</sup> compound. In order to collect more information about the redox changes of freshly deposited PB films, we have studied ultrathin films prepared both in the absence and in the presence of K<sup>+</sup> ions, paying particular attention to those prepared in K<sup>+</sup>-containing solutions, because of their potential analytical applications.

### *Behaviour of PB Films Prepared in the Absence of Additional K<sup>+</sup> Salt*

In the first series of experiments PB was deposited onto a gold-coated glass sensor by potentiostatic method from 0.06 M HCl solution containing  $2 \times 10^{-3}$  M K<sub>3</sub>[Fe(CN)<sub>6</sub>] and  $2 \times 10^{-3}$  M FeCl<sub>3</sub>. After deposition of a 30 nm thick PB coating, the modified electrode was rinsed with aqueous solution containing 0.1 M KCl and 0.01 M HCl. Then, it was characterised in an aqueous solution containing the same electrolytes at the same concentration, by combined SPR and cyclic voltammetric measurements. The electrode potential was first cycled between +0.40 and 0.00 V at different scan rates (v), in order to monitor the PB/PW redox system by cyclic voltammetry and by simultaneous recording of the SPR signal. The potential scans at any scan rates started from the open circuit potential, where no current flows. Cyclic voltammograms and corresponding SPR angle signals are depicted in Fig. 1. The reduction of PB to PW occurs in the potential region from +0.20 to 0.00 V. The electrochemical reduction process is accompanied by a change of both refractive index and colour, from deep blue to colourless. The PB films are very stable in this potential range and observed changes in the electronic spectrum are reversible, as reported in<sup>22-24</sup>. At the beginning of the cathodic sweep, the change of the SPR angle is negative (Fig. 1a, recorded at  $v = 5$  mV s<sup>-1</sup>). After passing a minimum, the SPR angle increases slowly at potentials more positive than those of PB reduction peak. When

the sweep is reversed, i.e. when the re-oxidation of PW to PB takes place, a sharp change in the SPR angle, with a minimum, is observed. Marked differences are present in the trace recorded at  $v = 100 \text{ mV s}^{-1}$ , as it can be seen in Fig. 1b.

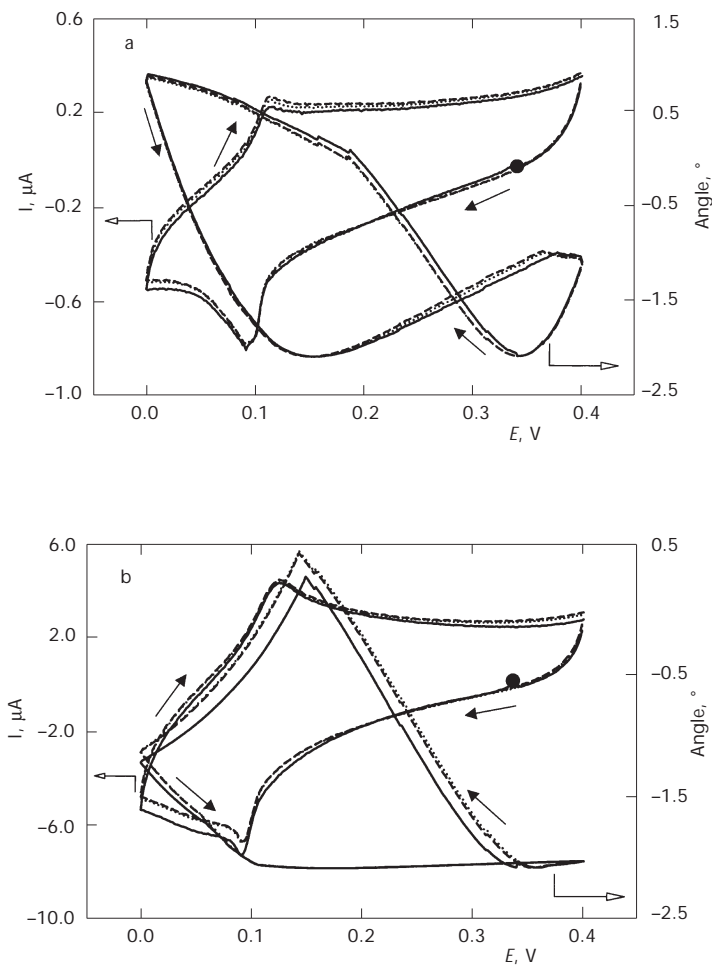


FIG. 1  
Cyclic voltammograms in 0.1 M KCl-0.01 M HCl, gold-coated glass electrode with PB film grown in the absence of  $\text{K}^+$  ions added ( $d = 30 \text{ nm}$ ), potential range from +0.40 to 0.00 V; ● starting potential in the first cycle. The ordinate axis on the right reports the changes in the SPR angle during potential cycling. a  $v = 5 \text{ mV s}^{-1}$ , b  $v = 100 \text{ mV s}^{-1}$ . — 1st scan, ..... 2nd scan, - - - 3rd scan

The behaviour of the PB films grown in the absence of additional  $K^+$  has been investigated also in neutral solutions containing 0.1 M  $KNO_3$ ; the PB/PW redox potential is shifted by ca. 100 mV. Tests at different scan rates have been performed. In Fig. 2 the voltammetric and SPR responses recorded during potential cycles at two selected scan rates are shown. In this

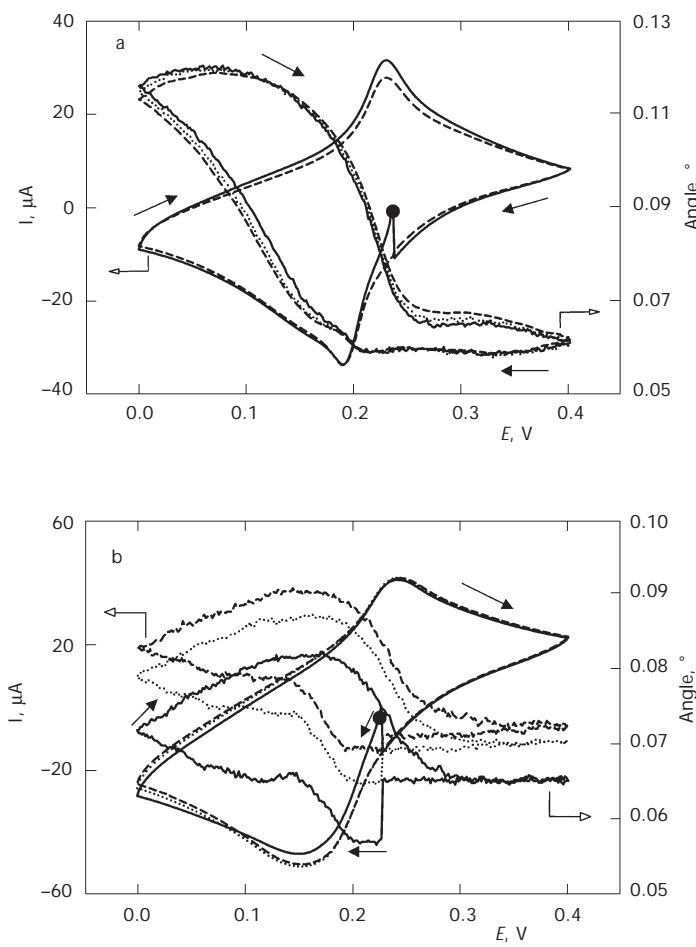


FIG. 2  
Cyclic voltammograms in 0.1 M  $KNO_3$ , gold-coated glass electrode with PB film grown in the absence of  $K^+$  ions added ( $d = 30$  nm), potential range from +0.40 to 0.00 V; ● starting potential in the first cycle. The ordinate axis on the right reports the changes in the SPR angle during potential cycling. a  $v = 20$  mV  $s^{-1}$ , b  $v = 100$  mV  $s^{-1}$ . — 1st scan, ..... 2nd scan, ---- 3rd scan

case, the SPR angle is almost constant in the potential interval from +0.40 to +0.20 V. Then, with the onset of the reduction process, the value of the SPR angle increases. Such behaviour has been observed at all scan rates applied in this solvent medium.

Comparing responses obtained in  $\text{KCl} + \text{HCl}$  with those in  $\text{KNO}_3$  solution yields a similarity of cyclic voltammetric curves, despite a well evident difference of SPR signals. This aspect evidences the notably interesting capability of the ESPR technique to highlight the effects not indicated by the electrochemical technique. In this case, the influence of the supporting electrolyte, i.e. the solvent, on the PB/PW redox system can be resolved. Furthermore, the difficulty to reach equilibrium at varying the applied potential is well evidenced by the ESPR in  $\text{KNO}_3$  solution at  $v = 100 \text{ mV s}^{-1}$ . The ESPR curves in subsequent scans are different, while voltammetric curves are equal.

Prolonged cycling in this medium causes decomposition of the PB film, as shown in Fig. 3, recorded on the same deposit as in Fig. 2. Before recording Fig. 3, the deposit was treated by continuous potential cycling for 2 h. The cyclic voltammogram resembles diffusion-controlled charge transfer process. The SPR signal dramatically changed as well, exhibiting very broad peaks with a quasi-sigmoidal shape, with maximum and minimum angle values located at the cathodic and anodic current peak potentials, respectively.

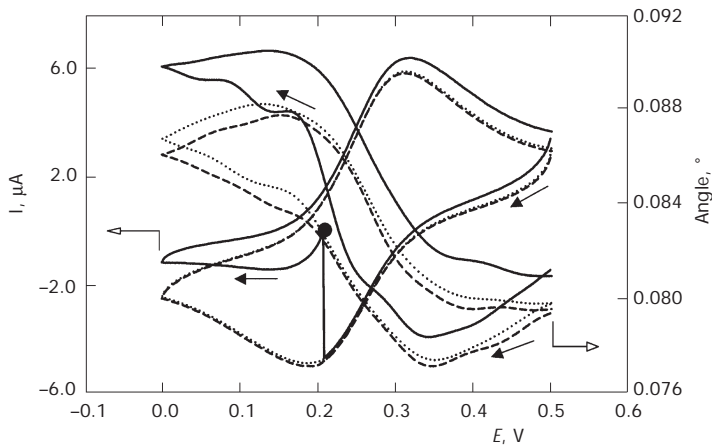


FIG. 3

Cyclic voltammograms in  $0.1 \text{ M } \text{KNO}_3$ , gold-coated glass electrode with PB film grown in the absence of  $\text{K}^+$  ions added ( $d = 30 \text{ nm}$ ), potential range from +0.50 to 0.00 V; ● starting potential in the first cycle. The ordinate axis on the right reports the changes in the SPR angle during potential cycling at  $50 \text{ mV s}^{-1}$ . — 1st scan, ..... 2nd scan, ---- 3rd scan

tively. The ESPR response changed from characteristics of electroactive adsorbed species to species in solution. This confirms that the stability of PB films, prepared in absence of additional  $K^+$ , is satisfactory in acidic solutions, while in neutral media slow dissolution of the films occurs. Similar results have been recently reported<sup>25</sup> on the behaviour of  $[Fe(CN)_6]^{3-}$ – $[Fe(CN)_6]^{4-}$  couple in neutral solutions.

### *Behaviour of PB Films Prepared in Presence of Additional $K^+$*

#### Cyclic Voltammetry

Ultrathin PB films have also been prepared in the presence of additional  $K^+$  ions, in 0.1 M  $K_2SO_4$  and 0.01 M  $H_2SO_4$ , with  $2 \times 10^{-3}$  M  $K_3[Fe(CN)_6]$  and  $2 \times 10^{-3}$  M  $FeCl_3$ . In this case, the stability of the film is enhanced. The thickness (6 nm) was lower than in previous case.

In Fig. 4 the first three scans on PB film in acidic solution containing 0.1 M  $K_2SO_4$  and 0.01 M  $H_2SO_4$  are depicted. The cyclic voltammetric responses overlap indicating good stability of the deposit. However, the ESPR signal reveals small changes in electro-optical properties during potential cycling. In this case, the ESPR response is different from that of PB films prepared in  $K^+$ -free solutions. It shows almost constant values at potentials

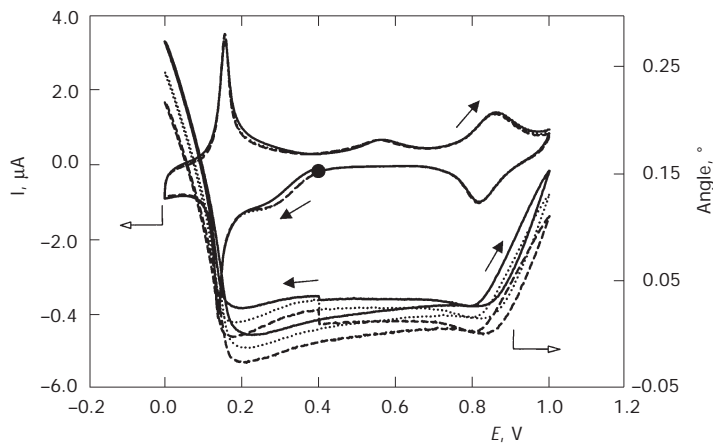


FIG. 4

Cyclic voltammograms in 0.1 M  $K_2SO_4$ –0.01 M  $H_2SO_4$ , gold-coated glass electrode with PB film grown in the presence of  $K^+$  ions added ( $d = 6$  nm), potential range from 0.00 to +1.00 V; ● starting potential in the first cycle. The ordinate axis on the right reports the changes in the SPR angle during potential cycling at  $v = 20$  mV s<sup>-1</sup>. — 1st scan, ..... 2nd scan, ---- 3rd scan

positive from reduction of PB, followed by a sharp increase near the peak potential. Compared with the  $I$ - $E$  curve in subsequent cycles, the ESPR signal (Fig. 4) reveals that the change of refractive index due to transformation of PB into its oxidised form (BG) is smaller than that for the change to the reduced form (PW).

An alternative approach to the study of ultrathin PB films by SPR technique consists in recording the reflectivity changes during potential cycling. Figure 5 shows the voltammograms and simultaneous reflectivity data (Fig. 5a), as well as the relevant time differential curves (Fig. 5b), re-

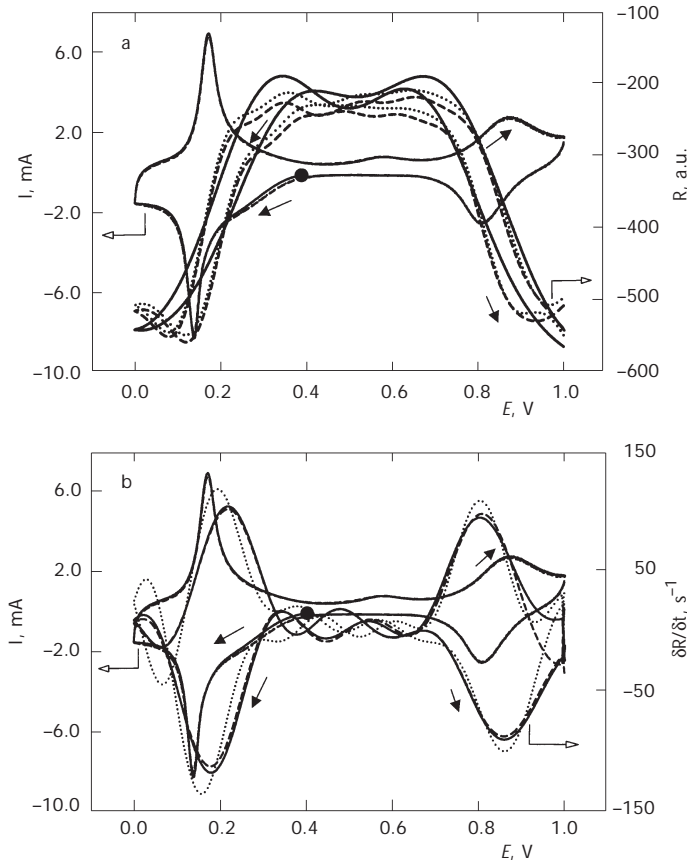


FIG. 5

Cyclic voltammograms in  $0.1 \text{ M } \text{K}_2\text{SO}_4$ - $0.01 \text{ M } \text{H}_2\text{SO}_4$ , gold-coated glass electrode with PB film ( $d = 6 \text{ nm}$ ), potential range from 0.00 to  $+1.00 \text{ V}$ ; ● starting potential in the first cycle,  $v = 50 \text{ mV s}^{-1}$ . The ordinate axis on the right reports the SPR reflectivity during potential cycling (a) and the time differential curves of the SPR reflectivity during potential cycling (b). — 1st scan, ..... 2nd scan, ---- 3rd scan

corded during both reduction and oxidation of PB. Figure 5a shows the reflectivity of reduced PB (i.e. of PW) about equal to that of oxidised PB (i.e. of BG). In the potential region within the values at which the PB/PW and PB/BG systems are located, a minimum of reflectivity is recorded.

By processing spectroelectrochemical data leading to the so-called voltabsorptometric curves<sup>29</sup>, we calculated the time dependence of differential curve of the reflectivity index, which was similar to that of corresponding cyclic voltammograms. It showed a couple of peaks centred at the formal redox potential of PB/PW and PB/BG, respectively, as can be seen from Fig. 5b. These results once more confirm that the *in situ* ESPR is particularly effective in detecting changes of the PB properties.

Subsequent potential cycles applied on PB film in the potential range from 0.00 to +1.00 V reveal a sufficient stability of the system, as can be seen from the cyclic voltammograms depicted in Fig. 6. A decrease of 14, 13, 9.5, and 13% for anodic and cathodic PB/PW peak currents or for anodic and cathodic PB/BG peak currents, respectively, is observed after 20 potential scans at  $v = 50 \text{ mV s}^{-1}$ . The corresponding changes of the ESPR signal are more pronounced, as it is evident from Fig. 6. In this case, a de-

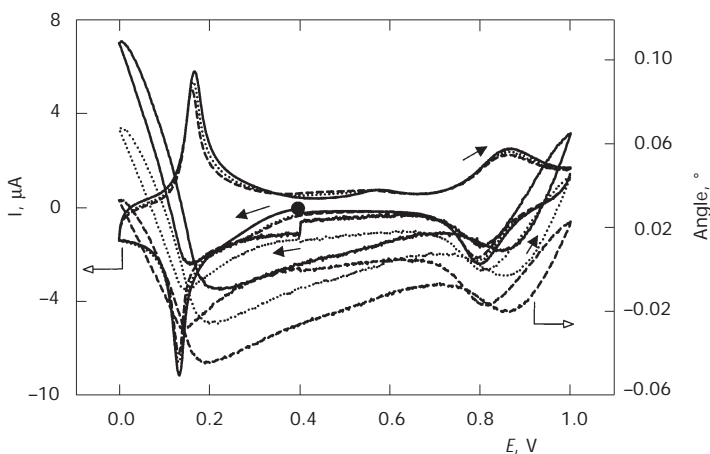


FIG. 6

Cyclic voltammograms in  $0.1 \text{ M K}_2\text{SO}_4$ – $0.01 \text{ M H}_2\text{SO}_4$ , gold-coated glass electrode with PB film ( $d = 6 \text{ nm}$ ), potential range from 0.00 to +1.00 V; ● starting potential in the first cycle,  $v = 50 \text{ mV s}^{-1}$ . The ordinate axis on the right reports the changes in the SPR angle during potential cycling. — 1st scan, ..... 10th scan, ----- 20th scan

crease of about 40% for the ESPR signal after 20 potential scans is observed. It is noteworthy that changes of the refractive index and, consequently, changes in the ESPR response, are higher for the PB/PW than for PB/BG system. Consequently, the sensitivity of an electrochemical-optical sensor based on this physical measurement is higher when working on the PB/PW, rather than on the PB/BG system, which is consistent with the electrochemical signal.

These results once more proved that the ESPR technique is more effective than cyclic voltammetry in revealing changes of the PB film: although information from both techniques are qualitatively in agreement, changes in electro-optical properties are pronounced. It must be underlined that the lowering of voltammetric and SPR signals during prolonged potential cycling within a wide potential range does not limit applicability of above mentioned ultrathin films.

The stability of PB films grown under these conditions has been checked also in  $\text{KNO}_3$ -containing solution. Similarly to what was reported in a previous Section, decomposition of PB films occurs over prolonged potential cycling, in agreement with literature reports<sup>9,11-15,24</sup>.

### Chronoamperometry

The effect of applied constant potential on the ESPR time response of PB films has been investigated using double potential step chronoamperometry. Both reduction and oxidation processes of PB films have been studied with this technique. For the reduction process, potential steps from +0.20 to -0.30 V, i.e. at least 0.20 V past the peak potential of the PB/ES system, have been applied in order to reach the diffusion-controlled mass transfer to the electrode. The slope of the  $\log I$  vs  $\log t$  plot yields ca. 0.6, not far from the theoretical value for a diffusion-controlled process. Under such experimental conditions, the full reduction of PB to PW takes place. The shape of the ESPR signal is quite similar to that of the current transient, as it can be seen from Fig. 7a, confirming that electrochemical change of PB to PW induces changes of its optical properties. Furthermore, the shape of the ESPR signal suggests that the full conversion of PB to PW takes place under these conditions, as expected taking into consideration the thickness of the films studied.

A different behaviour has been observed when the PB film is oxidised to BG: after potential jump from +0.20 to + 0.90 V, the slope of  $\log I$  vs  $\log t$  is ca. 0.74, and the ESPR signal does not reach a limiting value within the time of the experiment (Fig. 7b). Such behaviour is qualitatively in agree-

ment with lower oxidative current of PB, with respect to the reductive one. This suggests that conversion of PB to BG is not complete within the time scale used, differently from the conversion of PB to PW. This difference is not evidenced by chronoamperometric technique, thus once more underlining the usefulness of the electrode|modifier|electrolyte interfaces.

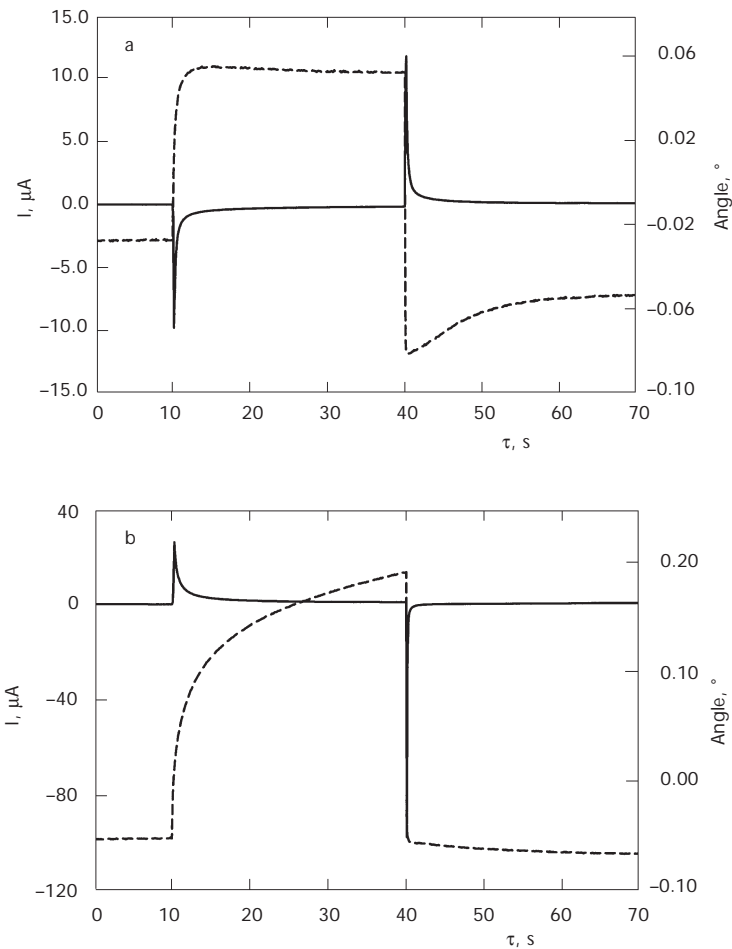


FIG. 7  
Double potential step at  $-0.30$  and  $+0.20$  V (a) and at  $+0.90$  V and  $+0.20$  V (b). PB film thickness  $d = 6$  nm,  $\tau$  is the time elapsed since the start of the experiment. — current, ----- SPR signal

## CONCLUSIONS

The SPR technique combined with cyclic voltammetry or chronoamperometry was found to indicate changes at the electrode|modifier|electrolyte interfaces, which are not detected by electrochemical techniques. Furthermore, information on the stability of PB films under different experimental conditions has been collected using the ESPR technique. In agreement with the current response, changes in the refractive index and, consequently, in the ESPR signal during potential cycling are more pronounced for the PB/PW than for the PB/BG system.

The results obtained clearly demonstrate that SPR is a particularly sensitive tool for *in situ* monitoring of minute changes of optical properties of ultrathin PB films deposited on the electrode surface.

*We are indebted to Eco Chemie B.V. and to Dr T. Frelink for providing the Autolab ESPRIT SPR instrument to us for six months. S. Lupu greatly appreciates the NATO-CNR fellowship supporting his six-month stay at the Department of Chemistry, University of Modena. Financial support of MIUR (Rome) (COFIN2002), is acknowledged.*

## REFERENCES

1. Buttry D. A., Ward M. D.: *Chem. Rev.* **1992**, *92*, 1355.
2. Green R. J., Frazier R. A., Shakesheff K. M., Davies M. C., Roberts C. J., Tendler S. J. B.: *Biomaterials* **2000**, *21*, 1823.
3. Homola J., Yee S. S., Gauglitz G.: *Sensors Actuators, B* **1999**, *54*, 3.
4. Baba A., Advincula R. C., Knoll W.: *J. Phys. Chem. B* **2002**, *106*, 1581.
5. Kang X., Jin Y., Cheng G., Dong S.: *Langmuir* **2002**, *18*, 1713.
6. Bailey L. E., Kambhampati D., Kanazawa K. K., Knoll W., Frank C. W.: *Langmuir* **2002**, *18*, 479.
7. Itaya K., Uchida I., Neff V. D.: *Acc. Chem. Res.* **1986**, *19*, 162.
8. Karyakin A.: *Electroanalysis* **2001**, *13*, 813.
9. Ogura K., Endo N., Nakayama M., Ootsuka H.: *J. Electrochem. Soc.* **1995**, *142*, 4026.
10. Karyakin A. A., Karyakina E. E., Gorton L.: *Anal. Chem.* **2000**, *72*, 1720.
11. Scharf U., Grabner E.: *Electrochim. Acta* **1996**, *41*, 233.
12. Totir N., Lupu S., Ungureanu E. M., Giubelean M., Stefanescu A.: *Rev. Roum. Chim.* **2001**, *46*, 1091.
13. Totir N., Lupu S., Ungureanu E. M., Iftimie N.: *Rev. Chim. (Bucharest)* **2001**, *2*, 23.
14. Lupu S., Mihailciuc C., Pigani L., Seeber R., Totir N., Zanardi C.: *Electrochim. Commun.* **2002**, *4*, 753.
15. Zhao H., Yuan Y., Adelolu S., Wallace G. G.: *Anal. Chim. Acta* **2002**, *472*, 113.
16. Feldman B. J., Murray R. W.: *Anal. Chem.* **1986**, *58*, 2844.
17. Siperko L. M., Kuwana T.: *J. Electrochem. Soc.* **1983**, *130*, 396.
18. Ludi A., Gudel H. V.: *Struct. Bonding (Berlin)* **1973**, *14*, 1.
19. Lundgren C. A., Murray R. W.: *Inorg. Chem.* **1988**, *27*, 933.

20. Mortimer R. J., Rosseinsky D. R.: *J. Chem. Soc., Dalton Trans.* **1984**, 2059.
21. Ellis D., Eckhoff M., Neff V. D.: *J. Phys. Chem.* **1981**, *85*, 1225.
22. Pyrasch M., Toutianoush A., Jin W., Schnepf J., Tieke B.: *Chem. Mater.* **2003**, *15*, 245.
23. Itaya K., Ataka T., Toshima S.: *J. Am. Chem. Soc.* **1982**, *104*, 4767.
24. Oslonovitch J., Li Y.-J., Donner C., Krischer K.: *J. Electroanal. Chem.* **2003**, *541*, 163.
25. Hamnett A., Higgins S., Mortimer R. S., Rosseinsky D. R.: *J. Electroanal. Chem.* **1988**, *255*, 315.